



Published in final edited form as:

Org Lett. 2018 September 21; 20(18): 5918–5921. doi:10.1021/acs.orglett.8b02584.

Comparative Studies of the Biosynthetic Gene Clusters for Anthraquinone-Fused Eneidiynes Shedding Light into the Tailoring Steps of Tiancimycin Biosynthesis

Xiaohui Yan^{#†}, Jian-Jun Chen^{#†}, Ajeeth Adhikari^{†,||}, Christiana N. Teijaro[†], Huiming Ge[†], Ivana Crnovcic[†], Chin-Yuan Chang[†], Thibault Annaval[†], Dong Yang[†], Christoph Rader^{||}, and Ben Shen^{*,†,‡,§}

[†]Department of Chemistry, The Scripps Research Institute, Jupiter, Florida 33458, United States

[‡]Department of Molecular Medicine, The Scripps Research Institute, Jupiter, Florida 33458, United States

[§]Natural Products Library Initiative at the Scripps Research Institute, The Scripps Research Institute, Jupiter, Florida 33458, United States

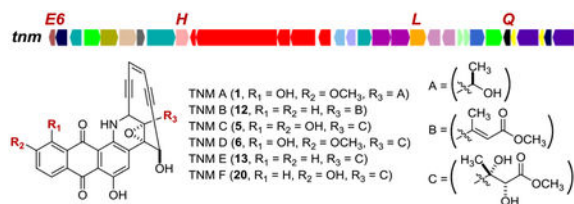
^{||}Department of Immunology and Microbiology, The Scripps Research Institute, Jupiter, Florida 33458, United States

[#] These authors contributed equally to this work.

Abstract

Comparative analyses of the four known anthraquinone-fused eneidiynes biosynthetic gene clusters identified four genes, *tnmE6*, *tnmH*, *tnmL*, and *tnmQ*, unique to the *tnm* gene cluster. Larger scale fermentation of both the *S. sp.* CB03234 wild-type and the *tnmH* and *tnmL* mutant strains resulted in the characterization of 20 new tiancimycin (TNM) congeners, including five eneidiynes. These findings enabled a proposal for the late stage of TNM biosynthesis featuring an intermediate possibly common for all anthraquinone-fused eneidiynes.

Graphical Abstract



*Corresponding Author: shenb@scripps.edu.

ASSOCIATED CONTENT

Supporting Information

The Supporting Information is available free of charge on the ACS Publications website at DOI: 10.1021/acs.orglett.8b02584.

General experimental procedures; Tables S1–S8, Figures S1–S156 (PDF)

The authors declare no competing financial interest.

The enediyne natural products have been classified into 9- or 10-membered subcategories according to the size of the enediyne cores.^{1–3} The 10-membered enediynes can be further divided into two subfamilies: the calicheamicin (CAL)-like enediynes and the anthraquinone-fused enediynes, including tiancimycin A (TNM A, **1**) from *Streptomyces* sp. CB03234,⁴ unciamycin (UCM, **2**) from *Streptomyces uncialis*,⁵ yangpumycin A (YPM A, **3**) from *Micromonospora yangpuensis*,⁶ and dynemicin (DYN, **4**) from *Micromonospora chersina*⁷ (Figure 1). While biosynthesis and engineering of the 9-membered enediynes have been greatly facilitated by the genetic amenability of selected producers with high enediyne titers,^{8–13} biosynthesis of the 10-membered enediynes remains poorly understood, mainly due to the lack of a model system with expedient genetic amenability, high enediyne titer, or combination of both.^{11,12}

Biosynthesis of anthraquinone-fused enediynes has received considerable attention since the discovery of **4** in 1989.⁷ Early isotope labeling studies in *M. chersina* revealed that both the enediyne core and the anthraquinone halves of **4** were of polyketide origin.¹³ A recent study suggested that the enediyne polyketide synthase (PKS) DynE8 may play a dual role in the biosynthesis of both halves of **4**.^{14,15} Both **3** and **4** are produced by *Micromonospora* species, which, in general, lack expedient genetic tools for *in vivo* studies, and **2** is produced by a *Streptomyces* species, but only on solid media with extremely low titer.⁵ We recently demonstrated that *S.* sp. CB03234 is genetically amenable⁴ and can produce **1** with high titer (~22 mg/L) in liquid fermentation,¹⁶ making it an ideal model system to study anthraquinone-fused enediyne biosynthesis.

The similarity in both structures and gene clusters of **1**–**4** (Figure 1, Figure S1) suggests a common pathway for anthraquinone-fused enediyne biosynthesis. The *dyn* and *ypm* gene clusters are similar to each other in both gene content and organization,⁶ harboring multiple genes that are absent in the *tnm* and *ucm* gene clusters.⁴ The *tnm* cluster contains all 28 genes in the *ucm* cluster, with four additional genes, *tnmE6*, *tnmH*, *tnmL*, and *tnmQ* (Figure 1, Figure S1), which encode a flavin reductase (TnmE6), a SAM-dependent methyltransferase (TnmH), a P450 hydroxylase (TnmL), and a protein of unknown function (TnmQ), respectively.⁴ Considering **1** as a 6-hydroxyl and 7-methoxyl congener of **2** (Figure 1), we initially proposed **2** as a biosynthetic intermediate en route to **1** in *S.* sp. CB03234. However, inactivation of *tnmH* in CB03234 afforded the *tnmH* mutant strain SB20002 that produced TNM C (**5**), an enediyne with an unexpected side chain appended to the enediyne core (Figure 2),⁴ suggesting a more complicated pathway for **1** biosynthesis.

In this study, we inactivated *tnmE6*, *tnmL*, and *tnmQ* individually in *S.* sp. CB03234 to afford the mutant strains SB20019 (i.e., *tnmE6*), SB20020 (i.e., *tnmL*), and SB20021 (i.e., *tnmQ*), respectively (Figures S2–S4). Fermentation of SB20019, SB20020, and SB20021, together with SB20002,⁴ as well as CB03234 as a control, showed that production of **1** was not affected in SB20019 and SB20021, indicative of functional redundancy, but abolished in SB20002 and SB20020, with concomitant accumulation of new metabolites (Figures 2, S5–S7). Complementation of the *tnmH* or *tnmL* mutation, by expressing a functional copy of *tnmH* (i.e., SB20022) or *tnmL* (i.e., SB20023) in trans, restored **1** production, excluding potential polar effects in the two mutants (Figure 2). We subjected the CB03234 wild-type (WT) and the SB20002 and SB20020 mutant strains to large-scale fermentation

(14 L each) and isolated, in addition to **1** and **5**, 20 new TNM congeners (6–25); their structures were established based on a combination of high-resolution MS and 1D and 2D NMR analyses (Tables S4–S8 and Figures S8–S156).^{4–7}

Six new TNM congeners (**6–11**), in addition to **1**, were isolated from the CB03234 WT (Figures 2, 3). Compound **6**, named TNM D, was characterized as a new enediyne with a side chain identical to TNM C (**5**)⁴ (Tables S4 and Figure S8). Compounds **7–11** were isolated as the cycloaromatized products, of which **7–9** were from **1**, while the enediyne form of **10** and **11** has yet to be isolated (Table S5 and Figure S13, S15). For **10** and **11**, the configuration of C-26 (*R*) and C-28 (*R*) was established through ROESY correlations between H-17 and CH₃-27 and between H-24 and H-28, respectively (Figures S11). Since cycloaromatization does not affect the stereochemistry at C-26 and C-28 (Figure S15), the stereochemistry of **6** could also be assigned as 26*R* and 28*R* based on the same biosynthetic origin (Figures 3, 4, S8).

Eight new TNM congeners (**12–19**) were isolated from the *tnmL* mutant strain SB20020 (Figures 2, 3, Tables S4, S6–S7, and Figures S8–S11), including two enediynes, named TNM B (**12**) and TNM E (**13**), both of which also possess a side chain attached to the enediyne core. The side chain of **12** features an α,β -unsaturated double bond, the trans configuration of which was assigned based on the absence of ROESY correlation between H-27 and H-28 (Figure S8). Compounds **14** and **15** are the cycloaromatized products of **12** (Figure S14). The side chain of **13** is identical to that of **5** and **6** (Table S4, Figure S14), and **17–19** are the cycloaromatized products of **13** (Figure S15). The stereochemistry of **13** can be similarly assigned as 26*R* and 28*R* on the basis of ROESY correlations between H-17 and CH₃-27 and between H-24 and H-28, respectively, observed for **17–19** (Figure S10). Compound **16** was unique among all the compounds isolated due to the presence of an additional F-ring, which is reminiscent of the structure of **4** (Figures 1A, S12, Table S8). The corresponding enediyne form of **16** was not isolated, however, in spite of extensive effort (Figures 4, S16). Since all the compounds isolated from SB20020 lack the hydroxyl group at C-6 and C-7, TnmL most likely catalyzes hydroxylation at both positions (Figure 4).

Six new TNM congeners (**20–25**), in addition to **5**,⁴ were isolated from the *tnmH* mutant strain SB20002 (Figures 2, 3, Tables S4, S7), including a new enediyne named TNM F (**20**) and five cycloaromatized products **21–25**. Compound **20**, which bears the same side chain as **5**, **6**, and **13**, was readily determined to be the 6-deshydroxyl congener of **5** (Table S4, Figure S8). Compounds **21** and **23** are the cycloaromatized products of **20**, and **22**, **24**, and **25** are the cycloaromatized products of **5** (Figure S15). The stereochemistry at C-26 and C-28 of both **20** and **5** can be similarly assigned as 26*R* and 28*R* on the basis of ROESY correlations between H-17 and CH₃-27 and between H-24 and H-28, respectively, observed for **22–25** (Figure S11). Since all congeners isolated from SB20002 feature a free hydroxyl group at C-7, TnmH most likely catalyzes *O*-methylation of the C-7 hydroxyl group. The fact that all congeners isolated possess a C-7 hydroxyl group would suggest that hydroxylation at C7 occurs before that at C6 (Figure 4)

Isolation and structural elucidation of the TNM congeners from the *S. sp* CB03234 WT and the SB20020 and SB20002 mutant strains enabled us to propose the post-PKS tailoring steps

for **1** biosynthesis (Figure 4). Thus, the tailoring steps start from a hexacyclic intermediate **26**, the identity of which was supported by the isolation of its cycloaromatized form **16** from the *tnmL* mutant of SB20020 (Figure S16). Since no other compounds isolated possess an intact F-ring, **26** must have first undergone F-ring cleavage to afford **12**, the α,β -unsaturated methyl ester side chain of which is subsequently dihydroxylated to yield **13**, as supported by the isolation of **12** and **13**, and their cycloaromatized products **14** and **15**, and **17–19**, respectively, from SB20020 (Figures S14, S15). Oxidation and *O*-methylation of the A-ring of **13** must have proceeded before the processing of its side chain, as evidenced by the isolation of **20**, and **5**, and their cycloaromatized products **21** and **23**, and **22–25**, respectively, from the *tnmH* mutant of SB20002 and **6** and **27**, as its cycloaromatized forms **10** and **11**, from the WT strain of CB03234 (Figure S15). TnmL and TnmH next serve as the candidates, catalyzing sequential hydroxylations at C-7 and C-6, and *O*-methylation of the hydroxyl group at C-7, respectively, although it is unclear if hydroxylation at C-6 (path a) or *O*-methylation of the hydroxyl group at C-7 (path b) occurs first, since both **5** and **27**, in its cycloaromatized form, have been isolated. Both paths converge to afford **6**, which, with its fully modified A-ring, undergoes the final steps of side chain processing to yield **1** (Figure 4).

In contrast, for biosynthesis of **2** in *S. uncialis* or **3** in *M. yangpuensis*, **26** would first undergo the same F-ring cleavage as **1** in *S. sp.* CB03234 to afford **13**. Subsequent processing of the side chain of **13**, however, would vary according to the substitutions on the A-ring, as exemplified by none, C-6 hydroxylation, or C-6 hydroxylation and C-7 methoxylation, respectively, en route to **2**, **3**, or **1** (Figure 4). Examination of the four gene clusters indeed revealed three sets of genes, *tnmI/ucmI/ypmI* encoding an oxidoreductase, *tnmK1/ucmK1/ypmK1* encoding a protein of unknown function, and *tnmM/ucmM/ypmM* encoding a Rieske iron–sulfur protein, that are absolutely conserved among the *tnm*, *ucm*, and *ypm* clusters but are absent from the *dyn* cluster (Figure S1).^{4,6,12} These enzymes serve as the candidates that catalyze the conversion of **26** to **13** and subsequently **13** to **1**, **2**, and **3**, respectively (Figure 4). The exact timing for each of the steps and the substrate specificity of these enzymes from each of the pathways, however, will have to be determined by in vitro characterizations.

Finally, the five new enediynes **5**, **6**, **12**, **13**, and **20** were tested for cytotoxicity against selected human cancer cell lines, including central nervous system (SF-295), melanoma (SKMEL-5), breast (MDA-MB-231 and SKBR-3), and nonsmall cell lung (NCI-H226), with **1** as a control.^{4,17} They exhibited a broad range of IC₅₀'s, with **1** as the most potent, followed by **6**, **13**, **12**, **5**, and **20** sequentially (Table 1). Since **1** differs from **6** only by the appended side chain, the slight decrease in potency suggests that the side chain plays a minor role in the cytotoxicity. In contrast, the increasing level of oxidation from **12**, **13**, to **6** correlated with an increase in potency, while a free hydroxyl group at C-7 appeared to be detrimental to the observed cytotoxicity, as exemplified by **5** and **20**.

In summary, comparative analysis of the *dyn*, *tnm*, *ucm*, and *ypm* biosynthetic gene clusters led to the identification of four genes unique to the *tnm* cluster (Figure 1). Inactivation of the four genes in *S. sp.* CB03234 yielded mutants that accumulated 20 new TNM congeners,

including five enediynes (Figure 3). The isolated TNM congeners provided new insights into the tailoring steps of **1** biosynthesis and enabled us to formulate a unified pathway for the four anthraquinone-fused enediynes, featuring **26** as a key common intermediate (Figure 4). These findings set the stage to investigate the mechanisms of how a common intermediate is channeled into the biosynthesis of each anthraquinone-fused enediyne. Engineering of the anthraquinone-fused enediyne biosynthetic machineries therefore promises to further expand the structural diversity, thereby defining the structure–activity relationship of the anthraquinone-fused enediynes, for anticancer drug discovery and development.

Supplementary Material

Refer to Web version on PubMed Central for supplementary material.

ACKNOWLEDGMENTS

This work is supported in part by National Institutes of Health Grants GM115575 (B.S.) and CA204484 (B.S. and C.R.). J.C. and I.C. were supported in part by postdoctoral fellowships from the State Key Laboratory of Applied Organic Chemistry, College of Chemistry and Chemical Engineering, Lanzhou University, and the Chinese Scholarship Council(201606185009), and the German Research Foundation, respectively. This is Manuscript No. 29708 from The Scripps Research Institute.

REFERENCES

- (1). Galm U; Hager MH; Van Lanen SG; Ju J; Thorson JS; Shen B *Chem. Rev* 2005, 105, 739–758. [PubMed: 15700963]
- (2). Van Lanen SG; Shen B *Curr. Top. Med. Chem* 2008, 8, 448–459. [PubMed: 18397168]
- (3). Liang Z-X *Nat. Prod. Rep* 2010, 27, 499–528. [PubMed: 20336235]
- (4). Yan X; Ge H; Huang T; Hindra; Yang D; Teng Q; Crnovcic I; Li X; Rudolf JD; Lohman JR; Gansemans Y; Zhu X; Huang Y; Zhao L-X; Jiang Y; Nieuwerburgh FV; Rader C; Duan Y; Shen B *mBio* 2016, 7, e02104–16. [PubMed: 27999165]
- (5). Davies J; Wang H; Taylor T; Warabi K; Huang X-H; Andersen RJ *Org. Lett* 2005, 7, 5233–5236. [PubMed: 16268546]
- (6). Yan X; Chen JJ; Adhikari A; Yang D; Crnovcic I; Wang N; Chang C-Y; Rader C; Shen B *Org. Lett* 2017, 19, 6192–6195. [PubMed: 29086572]
- (7). Konishi M; Ohkuma H; Matsumoto K; Tsuno T; Kamei H; Miyaki T; Oki T; Kawaguchi H; VanDuyne GD; Clardy JJ *Antibiot* 1989, 42, 1449–1452.
- (8). Liu W; Christenson SD; Standage S; Shen B *Science* 2002, 297, 1170–1173. [PubMed: 12183628]
- (9) (a). Kennedy DR; Gawron LS; Ju JH; Liu W; Shen B; Beerman TA *Cancer Res* 2007, 67, 773–781. [PubMed: 17234789] (b) Kennedy DR; Ju J; Shen B; Beerman TA *Proc. Natl. Acad. Sci. U. S. A* 2007, 104, 17632–17637. [PubMed: 17978180]
- (10). Liu W; Nonaka K; Nie L; Zhang J; Christenson SD; Bae J; Van Lanen SG; Zazopoulos E; Farnet CM; Yang CF; Shen B *Chem. Biol* 2005, 12, 293–302. [PubMed: 15797213]
- (11). Ahlert J; Shepard E; Lomovskaya N; Zazopoulos E; Staffa A; Bachmann BO; Huang K; Fonstein L; Czisny A; Whitwam RE; Farnet CM; Thorson JS *Science* 2002, 297, 1173–1176. [PubMed: 12183629]
- (12). Gao Q; Thorson JS *FEMS Microbiol. Lett* 2008, 282, 105–114. [PubMed: 18328078]
- (13). Tokiwa Y; Miyoshi-Saitoh M; Kobayashi H; Sunaga R; Konishi M; Oki T; Iwasaki SJ *Am. Chem. Soc* 1992, 114, 4107–4110.
- (14). Cohen DR; Townsend CA *Nat. Chem* 2017, 10, 231–236. [PubMed: 29359752]
- (15). Cohen DR; Townsend CA *Angew. Chem., Int. Ed* 2018, 57, 5650–5654.
- (16). Liu L; Pan J; Wang Z; Yan X; Yang D; Zhu X; Shen B; Duan Y; Huang YJ *Ind. Microbiol. Biotechnol* 2018, 45, 141–151.

(17). Nicolaou KC; Chen JS; Zhang H; Montero A *Angew. Chem., Int. Ed* 2008, 47, 185–189.

Author Manuscript

Author Manuscript

Author Manuscript

Author Manuscript

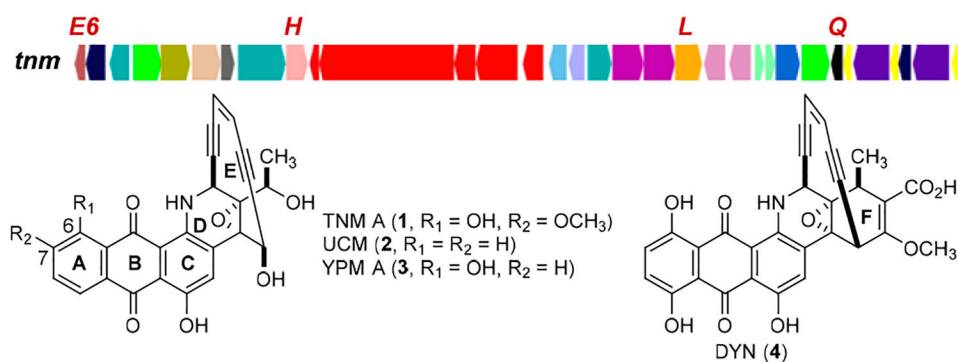


Figure 1. Structures of the four known anthraquinone-fused enediynes, TNM A (1), UCM (2), YPM (3), and DYN (4), and the *tnm* biosynthetic gene cluster from *S. sp.* CB03234 with the four genes inactivated in this study highlighted in red.

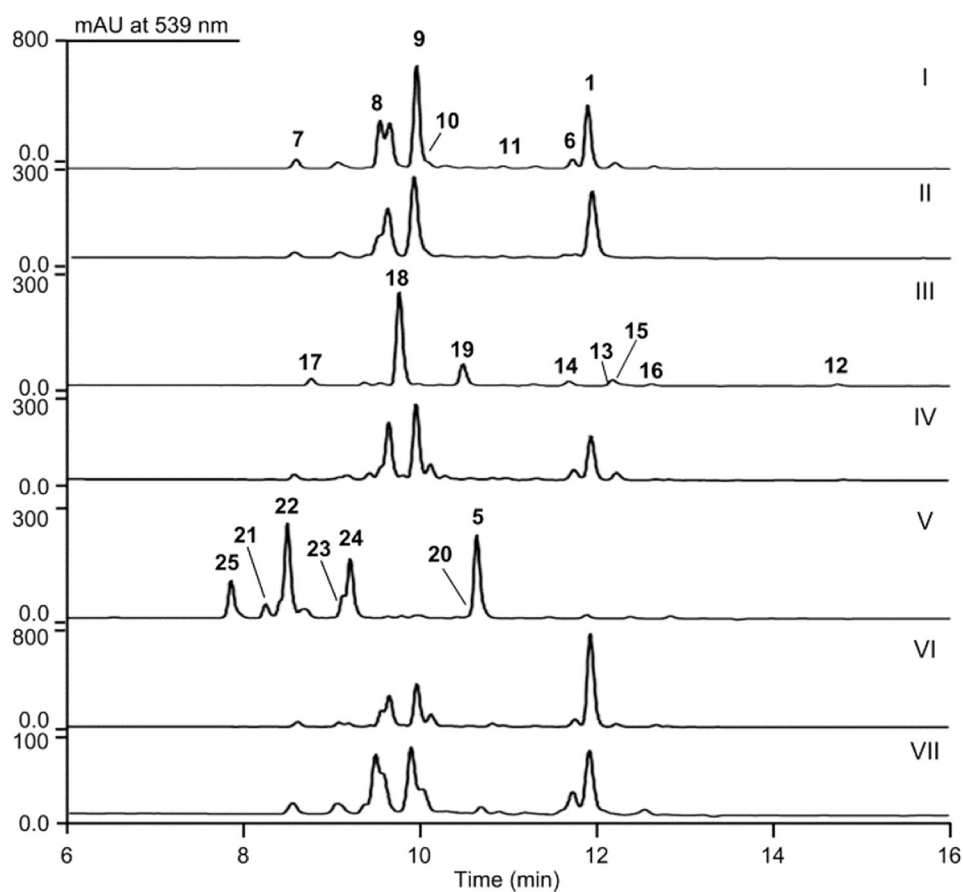


Figure 2. Metabolite profiles of the *S. sp.* CB03234 WT and mutant strains: (I) CB03234 WT; (II) SB20019 (*tnmE6*); (III) SB20020 (*tnmL*), (IV) SB20023 (*tnmL* + *tnmL*); (V) SB20002 (*tnmH*);(VI) SB20022 (*tnmH* + *tnmH*); (VII) SB20021 (*tnmQ*). See Figure 3 for structures of **1** and **5–25**.

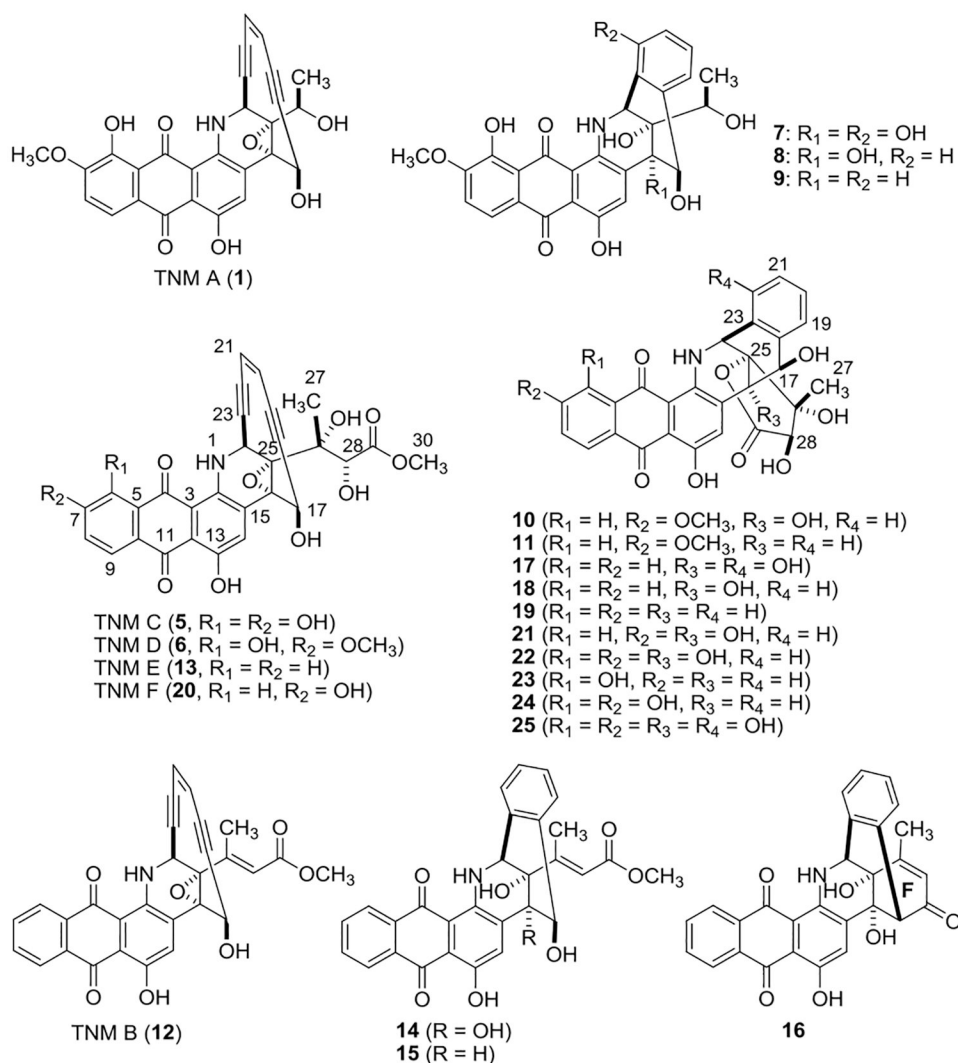


Figure 3. Structures of TNM A (1), TNM C (5), and the 20 new congeners (6–25) isolated from the *S.* sp. CB03234 WT and the SB20020 (*tmmL*) and SB20002 (*tmmH*) mutant strains.

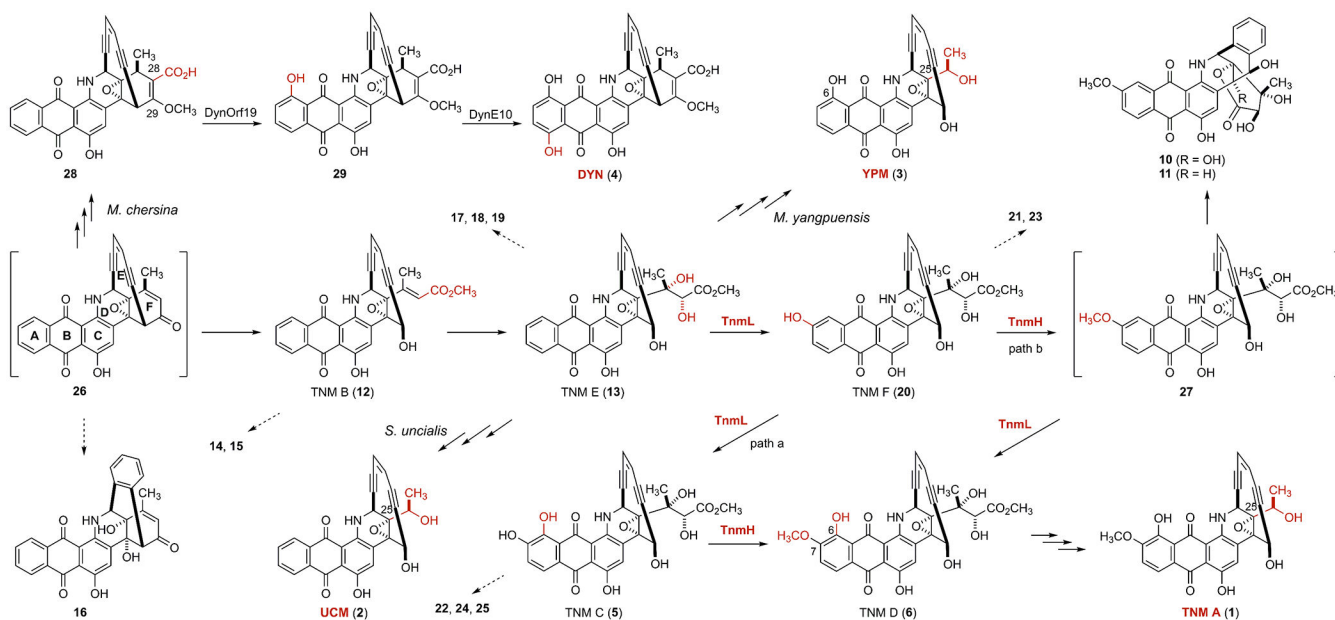


Figure 4.

Post-enediynes PKS tailoring steps for TNM A (1) biosynthesis in *S. sp.* CB03234 enabled the formulation of a unified biosynthetic pathway for all members of the family of anthraquinone-fused enediyne, DYN (4) in *M. chersina*, TNM (1), UCM (2) in *S. uncialis*, and YPM (3) in *M. yangpuensis*, featuring 26 as a key common intermediate. Groups transformed in each of the tailoring steps are highlighted in red. Intermediates in brackets are not isolated. Dashed arrows indicate shunt metabolites isolated.

Cytotoxicity (IC_{50} s in nM) of the Five New Enehydines (5, 6, 12, 13, 20), in comparison with TNM A (1), against Five Selected Human Cancer Cell Lines

Table 1.

cell line	SF-295	SKMEL-5	MDA-MB-231	SKBR-3	NCI-H226
1	0.83 ± 0.07	0.56 ± 0.12	1.0 ± 0.4	0.90 ± 0.19	17 ± 1
5	51 ± 9	22 ± 1	29 ± 1	22 ± 1	>100
6	2.2 ± 0.1	2.5 ± 0.1	2.1 ± 0.3	1.7 ± 0.1	31 ± 6
12	16 ± 2	13 ± 3	17 ± 3	14 ± 1	>100
13	8.0 ± 0.8	9.1 ± 1.6	8.4 ± 1.9	6.8 ± 0.2	>100
20	52 ± 2	24 ± 6	35 ± 4	16 ± 3	>100